Exchange interactions in $Ca_3Co_2O_6$ probed locally by NMR

G. Allodi,[1] P. Santini,[1] S. Carretta,[1] S. Agrestini,[2,3] C. Mazzoli,[4] A. Bombardi,[5] M. R. Lees,[6] and R. De Renzi[1]

[1]*Dipartimento di Fisica e Scienze della Terra, Università di Parma, Viale G. Usberti 7A, I-43124 Parma, Italy*

[2]*Laboratoire CRISMAT, UMR 6508, Boulevard du Maréchal Juin, 14050 Caen Cedex, France*

[3]*Max Planck Institute for Chemical Physics of Solids, Nöthnitzerstr. 40, 01187 Dresden, Germany*

[4]*Dipartimento di Fisica e unitá CNISM, Politecnico di Milano, Piazza L. da Vinci 32, I-20133 Milano, Italy*

[5]*Diamond Light Source Ltd., Rutherford Appleton Laboratory, Didcot OX11 0DE, United Kingdom*

[6]*Department of Physics, University of Warwick, Coventry CV4 7AL, United Kingdom*

(Received 20 December 2013; revised manuscript received 7 February 2014; published 3 March 2014)

We have measured the nuclear spin-lattice relaxation of ^{59}Co in the geometrically frustrated Ising-type spin-chain system $Ca_3Co_2O_6$ as a function of temperature and applied magnetic field. In the nearly-saturated ferrimagnetic and ferromagnetic regimes considered here, the field-dependent energy scales governing the spin-lattice relaxation rates reflect the energy cost of a spin flip in the Co ions adjacent to the probed nuclei. This results in a thermally activated form for the nuclear relaxation rates, which can be exploited as a local probe of the exchange interactions. In particular, the measurements enable the values of intra- and interchain exchange constants J_1, $J_2 + J_3$ to be directly extracted from the data. By using a quasi-one-dimensional model, we then determine the value of J_2 consistent with the spin-density-wave order observed in zero field.

DOI: 10.1103/PhysRevB.89.104401 PACS number(s): 76.60.−k, 75.30.Et, 75.30.Kz, 75.60.Jk

I. INTRODUCTION

The geometrically frustrated Ising-type magnet $Ca_3Co_2O_6$ has been the subject of growing fundamental interest in recent years, due to a complex phase diagram exhibiting a number of magnetic states as a function of temperature and applied magnetic field, which are a manifestation of the interplay of geometrical frustration and low dimensionality in the system [1]. The structure of $Ca_3Co_2O_6$ consists of spin-chains built up by the alternate stacking of high-spin ($S = 2$) Co^{3+} II (trigonal site) and nonmagnetic Co^{3+} I (octahedral site) along the c axis [2–4], and arranged into a triangular lattice [5]. The $S = 2$ spins are Ising-like due to a large easy-axis anisotropy. Exchange coupling is ferromagnetic (FM) and strong between neighboring Co^{3+} II ions along the chains, whereas it is antiferromagnetic (AF) and much weaker between chains [6,7].

The system orders magnetically at $T < T_N \approx 25$ K, as demonstrated by neutron diffraction [8,9]. The zero-field magnetic structure, however, had been a puzzle for over a decade, which has been solved only recently. The system orders in the form of a long-wavelength incommensurate spin density wave (SDW) [10,11], but at lower temperature this phase becomes metastable [11–13] and the long-range order shows an unprecedented ultraslow transformation into a commensurate AF structure with a completely different translational symmetry [14].

A magnetic field applied along the c axis first stabilizes ferrimagnetic (FI) structures, and eventually a full FM order at higher field intensity ($B \gtrsim 3.5$ T). However, the phenomenology is clear only at intermediate temperatures ($5\ \mathrm{K} < T < T_N$), where the FI structure is a simple up-up-down spin arrangement of the three chains, each with an intrachain FM order [6,15]. At lower temperatures, the $M(H)$ curves exhibit a strongly hysteretic multistep behavior, indicative of more complex magnetic configurations [6,16–19]. Theoretical models predict a number of superstructures of the spin chains as a function of the applied field, qualitatively reproducing the magnetization steps [20–22].

The peculiar phenomenology of $Ca_3Co_2O_6$ results from three main ingredients: (i) the large FM intrachain coupling J_1 (see Fig. 1), favoring 1D Ising correlations of longer and longer range as T drops below J_1/k_B. (ii) The AF character of the total coupling between adjacent chains, $J_2 + J_3$ [see Eq. (1) below], which makes the triangular arrangement of these nearly FM chains magnetically frustrated. (iii) The presence of two distinct interchain coupling constants. The associated effective field felt by each individual chain can stabilize AF intrachain correlations of very long wavelength with respect to the FM ones typical of isolated chains [point (i)].

In spite of the high degree of characterization of $Ca_3Co_2O_6$, a precise determination of all exchange constants is still lacking. This hampers a satisfactory understanding of the observed phenomenology, e.g., the zero-field SDW and how it evolves into a commensurate order at low T. A constant $(J_2 + J_3)/k_B$ of the order of 2 K can be estimated by the value of the critical field for the FI-FM transition, whereas the situation for the intrachain coupling J_1 is unclear. For a strictly 1D Ising system, macroscopic measurements would easily and directly yield J_1. Here, however, complex 3D effects appear at low T, while the simple Ising character of the spins is lost at higher T (for $T \gtrsim 50$ K the entropy per spin exceeds $k_B \ln 2$ [23]), and the whole set of atomic Co^{3+} II states needs to be modeled in detail. Thus, fitting spin-Hamiltonians to high-T macroscopic measurements provides only indirect and not univocal information on J_1. For instance, $J_1/k_B \simeq 170$ K [in the notation of Eq. (1)] is deduced by modeling the heat capacity maximum around 100 K with an $S = 2$ Ising Hamiltonian [23], whereas $J_1/k_B \simeq 30$ and $J_1/k_B \simeq 24$ K are obtained by interpreting susceptibility measurements with a three-states model [24] and with a classical Heisenberg model, respectively [25]. Estimations based on *ab initio* calculations yield $J_1 \simeq 70$–90 K [3,26].

The most powerful tool to extract the values of exchange constants is usually inelastic neutron-scattering (INS) as theoretical models (e.g., spin-wave or spinon models) can be directly fitted to the observed low-energy dynamics. Here,

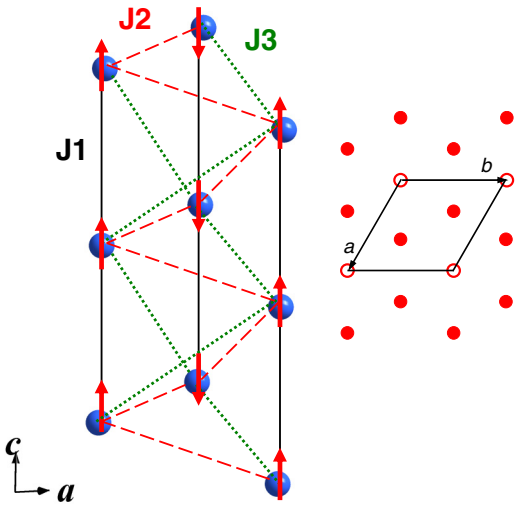

FIG. 1. (Color online) Magnetic couplings between Co spins: intrachain FM coupling J_1 and interchain AF couplings J_2 and J_3. The FI structure for the spins is illustrated. The projection of the chains in the ab plane forms a hexagonal lattice. Empty (filled) dots represent spin-up (spin-down) chains in the FI state.

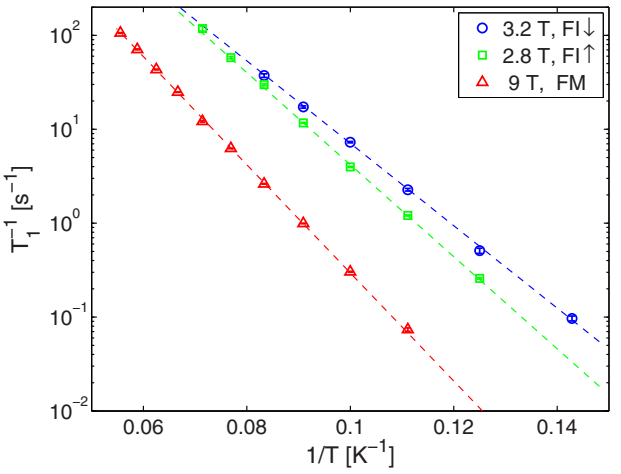

FIG. 2. (Color online) Spin-lattice relaxation rates T_1^{-1} vs $1/T$ in the majority (squares) and the minority (circles) spin chains of the FI phase and in the FM phase (triangles). Dashed lines are best fits to the Arrhenius law.

however, the Ising character of the Co^{3+} II pseudospins makes neutrons unable to flip them and to probe their excitation spectrum directly. A branch of quasi-one-dimensional excitations out of the Ising subspace has been recently identified around 30 meV by high-energy INS [27]. These results have been interpreted by a model of interacting $S = 2$ spins with easy-axis anisotropy D. Using a spin-wave approximation yields an estimate for $J_1 + D$, but not of J_1 and D separately.

In this work, we exploit NMR measurements as a local probe for the energy cost of a spin flip. We report the full dependence of the spin-lattice relaxations of ^{59}Co at site I as a function of temperature and applied magnetic field and we show that an Arrhenius law is obeyed throughout the intermediate temperature range at all fields, irrespective of the relative order of the spin chains (majority- and minority-FI, FM). From the measured field-dependent activation energies, the intrachain J_1 and interchain $J_2 + J_3$ exchange constants are directly accessed. By using a quasi-one-dimensional mean field model, we then determine the values of J_2 and J_3 consistent with the observed incommensurate ordering [14].

II. EXPERIMENTS

Experiments were carried out on a single crystal in a variable magnetic field nearly parallel to the c axis. Details of the sample preparation and the experimental apparatus are available in Ref. [28]. We recall that two distinct septets of quadrupole-split lines at resonance fields $B_{\rm nuc} \approx B_{\rm ext} \pm |B_{\rm int}|$ probe the majority spin-up and the minority spin-down chains of the FI structure, respectively, while a single septet, offset by a positive $B_{\rm int}$ from the applied field $B_{\rm ext}$, is detected in the FM phase. Here, the internal field $B_{\rm int}$, of the order of 1 T, is the resultant dipolar field from the surrounding Co II spins. Spin-lattice relaxations were measured by the recovery of the nuclear magnetization following a fast saturation of the central transition. The corresponding T_1^{-1} rates were obtained as the best-fit parameters to the multiexponential law of Eq. (B2) in Ref. [28].

Spin lattice relaxation rates in representative external fields, either in the FI ($B_{\rm ext} < B_{c2} \approx 3.6$ T) or in the FM phase ($B_{\rm ext} > B_{c2}$), are plotted on a semilogarithmic scale in Fig. 2 versus reciprocal temperature. The Arrhenius plots demonstrate the thermally activated dependence $T_1^{-1} = T_\infty^{-1} \exp(-\Delta/T)$, which is followed, in both phases and spin-chain orientations, over temperature intervals corresponding to a T_1 variation by three decades. Experimental rates deviate from the activated behavior at lower temperature, where a competing relaxation channel effectively shunts the extrapolated Arrhenius-law rates, which become vanishingly small. In contrast, at higher temperature, the signal is lost due to an exceedingly short spin-spin relaxation time T_2.

The dependence of the activation energy Δ on $B_{\rm ext}$ in the three magnetic environments (denoted with the $\uparrow$, $\downarrow$, and FM subscripts for the majority and minority FI chains, and the FM phase, respectively) is plotted in Fig. 3. The minority FI signal could only be accessed over a narrow field interval from 2.2 T up to B_{c2}, because of resonance frequencies lower than the low-frequency cutoff of our spectrometer (≈10 MHz) at lower fields, due to the antiparallel composition of $B_{\rm int}$ with $B_{\rm ext}$ at this site. Nevertheless, the negative slope of $\Delta_{\rm FI,\downarrow}$, opposite in sign to that of $\Delta_{\rm FI,\uparrow}$ and $\Delta_{\rm FM}$, is apparent from the figure.

The thermally activated T_1^{-1} rates indicate a gap in the spectrum of the electronic excitations responsible for the nuclear spin-lattice relaxation, and its field dependence clearly proves its magnetic origin. Given the nearly-saturated character of the investigated FI and FM regimes, we expect relevant excitations to be single spin flips in an almost frozen environment. The gap then monitors the value of the total (external plus internal) field at the spin site, thus providing a direct measurements of exchange constants. In this framework, the component of Δ linear in $B_{\rm ext}$ would be proportional to the magnetic moment μ, which is coupled to the field by a Zeeman term $-\mu B_{\rm ext}/k_B$ (in temperature units). Indeed, unconstrained fits of Δ to straight lines yield slope values $d\Delta_{\rm FM}/dB_{\rm ext} = 7.1(4)$ K/T,

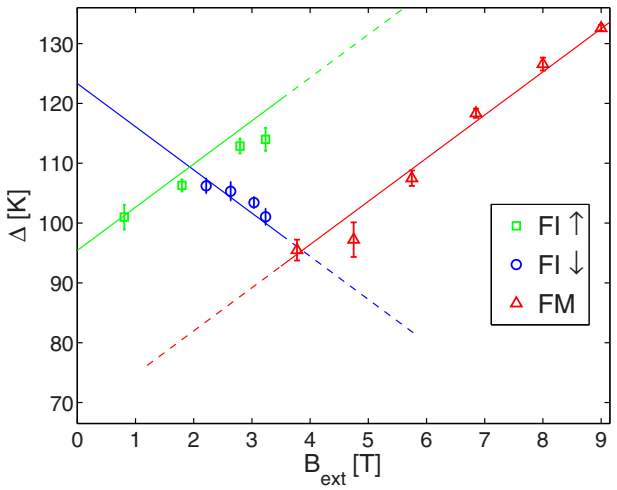

FIG. 3. (Color online) Activation energy of T_1^{-1}, in the units of temperature, in the majority and minority FI chains (squares and circles, $B_{\rm ext} < 3.5$ T) and in the FM chains (triangles, $B_{\rm ext} > 3.5$ T), as a function of the applied magnetic field. Solid lines are best fits to Eq. (2).

$d\Delta_{\rm FI,\uparrow}/dB_{\rm ext} = 6(1)$ K/T, and $d\Delta_{\rm FI,\downarrow}/dB_{\rm ext} = -5(3)$ K/T in the three magnetic surroundings. These values are in good quantitative agreement with ± 7.05 K/T, corresponding to a moment $\pm 10.5\,\mu_B$, as in the case of the total flip of a Co^{3+} spin from its ground-state value $\pm\mu = \pm 5.25$ [2,28] to $\mp gS$.

While the slope of the $\Delta(B_{\rm ext})$ curves reflects the Zeeman contribution to the energy cost of a spin flip, the internal field contribution fixes the offset of these curves. Retaining exchange integrals J_1, J_2, J_3 up to third nearest neighbors, the Hamiltonian for the Ising spin system in a longitudinal external field has the form

$$\mathcal{H} = \sum_k \Big[-\sum_\alpha J_1\, s_{k,\alpha} s_{k+1,\alpha} - \sum_{\langle\beta,\alpha\rangle} \big(J_2\, s_{k,\alpha} s_{k\pm 1/3,\beta} + J_3\, s_{k,\alpha} s_{k\pm 2/3,\beta} \big) - \sum_\alpha \mu s_{k,\alpha} B_{\rm ext} \Big], \quad (1)$$

where $s_{k,\alpha} = \pm 1$ and $\mu = gS\mu_{\rm B}$. k is an intrachain index and α, β are chain indices; the fractional k values account for the translation of the two neighboring chains α, β, whose relative Co^{3+} positions are shifted by $\pm$ one third of a Co II–Co II distance along the c axis. From Eq. (1), the cost in energy of a spin reversal process at $T \to 0$ (i.e., $s_{k,\alpha} = \pm 1$ as appropriate for the ground state) is calculated as

$$\begin{aligned} \Delta_{\rm FM} &= 4[J_1 + 3(J_2 + J_3)] + 2\mu B_{\rm ext}, \\ \Delta_{\rm FI,\uparrow} &= 4J_1 + 2\mu B_{\rm ext}, \\ \Delta_{\rm FI,\downarrow} &= 4[J_1 - 3(J_2 + J_3)] - 2\mu B_{\rm ext}. \end{aligned} \quad (2)$$

In Fig. 3, the solid lines are a global fit of the experimental Δ to Eq. (2), with the two exchange constants J_1, $J_{23} \equiv J_2 + J_3$, and the moment μ as free parameters. The fit is reasonably accurate (normalized $\chi^2 = 2$) and correctly yields a moment of $\mu = 5.3(2)\mu_B$, in agreement with the saturation value of the macroscopic magnetization [18,28]. Best fit values for the exchange constants are $J_1/k_B = 23.9(2)$ K and $J_{23}/k_B = -2.3(2)$ K. The value of J_{23} is in line with that expected from the location of the FI-FM transition. As far as J_1 is concerned, it is of the same order as the transverse exchange constant $J_\perp$ which determines the dispersion of the $M = \pm 2 \to M = \pm 1$ transition (bringing Co ions out of the Ising subspace). The fit of a spin-wave model to INS spectra yielded $J_\perp/k_B \simeq 19.5$ K [27]. Thus we deduce that the anisotropy between longitudinal (J_1) and transverse ($J_\perp$) exchange couplings in the full Heisenberg model for $S = 2$ spins is of the order of 20%.

III. MODEL

The description sketched above for the nuclear relaxation process can be validated by the Glauber model for the dynamics of an Ising spin system [29,30]. This model provides an effective representation of single-ion relaxation processes in the Ising subspace. These processes physically result from the modulation of the crystal field by phonons and are defined within the full manifold of Co II states. However, as long as Co spins are in the Ising regime (i.e., only the ground doublet of Co II ions is thermally populated), they can be parametrized by a flip probability per unit time for the Ising pseudospins. Such flip processes of the spins are felt by nearby Co I nuclei as a variation of the local hyperfine field, which has been shown in Ref. [28] to be of purely dipolar nature. Anyway, the results of this section do not depend on the precise nature of the hyperfine field (i.e., dipolar or transferred), apart from an inconsequential redefinition of the prefactor in Eq. (4). Time fluctuations of the local field at Co I nuclei $\mathbf{H}_{\rm dip}$ result in longitudinal nuclear relaxation:

$$\frac{1}{T_1} \propto \int_{-\infty}^{\infty} dt e^{i\omega_L t} \langle H_x(t)H_x(0) + H_y(t)H_y(0)\rangle, \quad (3)$$

where $\mathbf{H} = \mathbf{H}_{\rm dip} - \langle \mathbf{H}_{\rm dip}\rangle$, ω_L is the Larmor frequency, and z is the direction of the applied field. We call z' the direction of the Co chains in the crystal. The dominant contribution to $\mathbf{H}$ at the nonmagnetic Co I sites on a given chain comes from the spins of neighboring Co II ions belonging to the same chain. Since these Ising moments lie along z', if $z \equiv z'$ $\mathbf{H}//z$ by symmetry and $T_1^{-1} \to 0$:

$$\langle H_\alpha(t)H_\alpha(0)\rangle \propto R^{-6} \sin^2\theta \sum_{i,j=1}^{2} \langle \delta s_i(t)\delta s_j(0)\rangle, \quad (4)$$

where $\delta s = s - \langle s\rangle$, $\alpha = x, y$ and θ is the angle between z and z'. Labels i and j indicate the two neighboring Co II spins at distance R from the Co I nucleus. A sizable θ dependence of $1/T_1$ has indeed been found in Ref. [28]. In the present work, $\theta \sim 3^o$.

The dynamical spin correlations in Eq. (4) result from the flip processes of the Ising spins. Within the Glauber model the flip probability per unit time for the pth spin is

$$W_p(s_p) = \frac{1}{2\tau}(1 - s_p \tanh \beta E_p), \quad (5)$$

where the characteristic time τ is a parameter and the local field E_p is

$$E_p = \mu B_p + \sum_r J_{pr} s_r, \quad (6)$$

with B_p the external field on s_p, J_{pr} the Ising coupling between s_p and s_r. In the following, we adopt the mean-field approximation (MFA) for the dynamics [30], yielding

$$\tau \frac{d}{dt}\langle s_p\rangle = -\langle s_p\rangle + \tanh\beta(\mu B_p + \sum_r J_{pr}\langle s_r\rangle). \quad (7)$$

The MFA is reasonable in the regime investigated here of nearly saturated configurations (i.e., $|\langle s_p\rangle| \simeq 1$). We obtain dynamical spin correlations by calculating the nonlocal dynamical susceptibility $\chi(i,j;\omega)$ and using the fluctuation-dissipation theorem,

$$S_{ij}(\omega) \equiv \int_{-\infty}^{\infty} dt\ e^{i\omega t}\langle \delta s_i(t)\delta s_j(0)\rangle = \frac{2}{\beta\omega}\chi''(i,j;\omega). \quad (8)$$

The MFA Glauber equations lead to a random-phase-approximation form for the dynamical susceptibility, which can be deduced by calculating from Eq. (7) the time evolution in the presence of a small oscillating magnetic field. For instance, for the FM phase,

$$\chi(\mathbf{q},\omega) = \frac{\chi(\mathbf{q})}{1 - i\omega\tau(\mathbf{q})}, \quad \chi(\mathbf{q}) = \frac{\chi_1}{1 - J(\mathbf{q})\chi_1}, \quad \tau(\mathbf{q}) = \frac{\tau}{1 - J(\mathbf{q})\chi_1}, \quad (9)$$

where the wave-vector-dependent static susceptibility $\chi(\mathbf{q})$ and relaxation times $\tau(\mathbf{q})$ are given in terms of Fourier-transformed spin-spin couplings and of the single-spin static susceptibility χ_1,

$$\chi_1 = \beta(\langle s^2\rangle - \langle s\rangle^2) \xrightarrow{T\to 0} 4\beta e^{-\beta\Delta_{\rm FM}}, \quad (10)$$

where $\Delta_{\rm FM}$ is given in Eq. (2). Hence, as $T \to 0$ spin fluctuations are fast as all characteristic times $\tau(\mathbf{q})$ tend to τ. The dynamics become single-site in the sense that spatial correlations are lost and $\chi(\mathbf{q},\omega)$ reduces to the on-site ($\mathbf{q}$-independent), single-spin dynamical susceptibility in the static molecular field:

$$\chi(\mathbf{q},\omega) \xrightarrow{T\to 0} \frac{\chi_1}{1 - i\omega\tau}[1 + \mathcal{O}(\beta e^{-\beta\Delta_{\rm FM}})]. \quad (11)$$

The resulting two-spin correlations in Eq. (8) are

$$S_{ij}(\omega) = e^{-\beta\Delta_{\rm FM}}\frac{8\tau}{1+\omega^2\tau^2}\delta_{ij} + \mathcal{O}(J_1\beta e^{-2\beta\Delta_{\rm FM}}), \quad (12)$$

and therefore asymptotically,

$$\frac{1}{T_1} \propto e^{-\beta\Delta_{\rm FM}}\frac{\tau}{1+\omega_L^2\tau^2}. \quad (13)$$

This is just the expression fitted to the data in Fig. 2. The slowing-down of the nuclear spin dynamics as $T \to 0$ thus reflects the exponential decrease with T of the amplitude of spin fluctuations, whose relaxation time τ is fast and T-independent.

Similar results are obtained in the FI phase by a two-sublattice calculation. Again, spin fluctuations are local at low T. Their amplitude reflects the gap $\Delta_{\uparrow,\downarrow}$ [Eq. (2)] characterizing the spin chain probed by NMR:

$$\left(\frac{1}{T_1}\right)_{\uparrow,\downarrow} \propto e^{-\beta\Delta_{\uparrow,\downarrow}}\frac{\tau}{1+\omega_L^2\tau^2}, \quad (14)$$

as assumed in the fits in Fig. 3. We stress again that the expressions derived above are only valid in the regime considered here where the FM and FI phases are close to saturation. More complex effects must be accounted for at lower T or close to the FI-FM transition where slow out-of-equilibrium dynamics result in magnetization steps or hysteresis.

Having determined J_1 and $J_{23} = J_2 + J_3$, we now check whether these values are consistent with the observed transition to an incommensurate SDW in zero field. Calculations where the MFA is applied to all interactions in Eq. (1) lead to a large overestimation of T_N. For the given values of J_1 and J_{23}, the MFA equations for the first ordered state [31,32] yield the correct spin modulation for $J_2/k_B \simeq -1.24$ K, but with T_N as large as 55 K. This is not unexpected in view of the quasi-one-dimensional character implied by the hierarchy of exchange constants. In zero applied field, the associated short-range order leads to a removal of a large part of the magnetic entropy above T_N [23], an effect not accounted for in the MFA. To overcome this problem, we have performed calculations where the MFA is only applied to the interchain coupling terms (proportional to J_2 and J_3), whereas the intrachain coupling is included exactly by the analytic solution of the one-dimensional Ising model. In particular, the wave-vector-dependent static susceptibility of an Ising chain [30],

$$\chi_{\rm 1D}(q,T) = \beta\frac{1}{\cosh 2\beta J_1}\frac{1}{1 - \cos q\tanh 2\beta J_1}, \quad (15)$$

implies a transition from the paramagnetic to a modulated structure with $\mathbf{k} = 2\pi(\frac{\Delta}{3},\frac{\Delta}{3},\frac{\Delta}{3})$ (in the rhombohedral setting) at a temperature T_N given by

$$\chi_{\rm 1D}^{-1}[\pi(\Delta-1),T_N] = 6\left[J_3\cos\frac{2\pi\Delta}{3} - J_2\cos\frac{\pi\Delta}{3}\right]. \quad (16)$$

The resulting values of T_N are reported in Fig. 4 with fixed J_1 and J_{23}, as a function of J_2 and Δ. For a given J_2, the

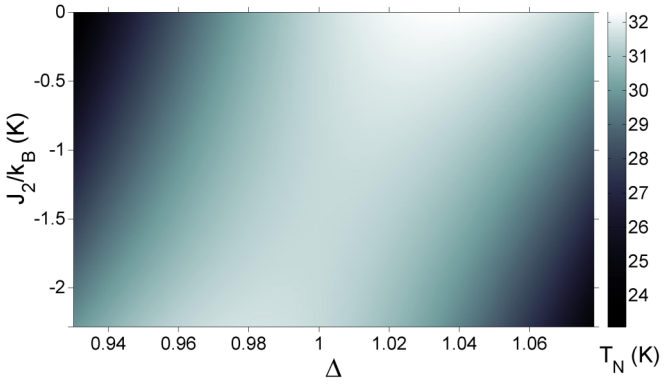

FIG. 4. (Color online) Intensity plot showing the transition temperature to the modulated phase in vanishing external field, as a function of J_2 and of the ordering wave vector (in reduced units). The quasi-one-dimensional model of Eq. (16) has been used, fixing $J_1/k_B = 23.9$ K and $(J_2 + J_3)/k_B = -2.3$ K. The observed wave vector is 1.01, corresponding to a wavelength of about 200 Co spins [11].

actual ordering wave vector is the one characterized by the largest T_N. The observed modulation $\Delta \simeq 1.01$ then implies $J_2/k_B \simeq -1.1$ K and hence $J_3/k_B \simeq -1.2$ K, for which $T_N \simeq 31.5$ K. This value is in very good agreement with the observed transition temperature (25 K), an overestimation of the order of 20% being expected in view of the MFA decoupling still used for J_2 and J_3 terms.

The spin density wave has been observed to become unstable at temperatures $T \lesssim 12$ K, where a commensurate stripelike antiferromagnetic phase sets in Ref. [14]. In fact, the exchange energy of this phase was calculated to be the lowest, whereas the phase is unfavorable at high T [32]. Even within the present quasi-1D framework the stripe phase does not appear as the first ordered state. In fact, its transition temperature is calculated from

$$\chi_{1D}^{-1}(0,T_s) = -2(J_2 + J_3), \tag{17}$$

yielding $T_s \simeq 27$ K $< T_N$.

IV. CONCLUSION

In conclusion, we have exploited measurements of the nuclear spin-lattice relaxation rate as a local probe to extract the values of the exchange constants in $Ca_3Co_2O_6$. In the regime of ferrimagnetic and ferromagnetic configurations close to saturation considered here, the relaxation time of Co-I nuclei directly reflects the energy cost for flipping an adjacent Co-II spin. Hence, by extracting from the data the field dependence of the energy-scale setting the thermally activated behavior of $1/T_1$, we have been able to deduce $J_1/k_B \simeq 23.9$ K and $(J_2 + J_3)/k_B \simeq -2.3$ K. These results have been validated by calculations using the Glauber model for the spin dynamics. We have then used a quasi-one-dimensional model to determine the value of $J_2/k_B \simeq -1.1$ K consistent with the spin-density-wave order observed in zero field.

ACKNOWLEDGMENT

Useful discussions with M. G. Pini are gratefully acknowledged.

[1] Y. B. Kudasov, A. S. Korshunov, V. N. Pavlov, and D. A. Maslov, Phys. Usp. **55**, 1169 (2012).
[2] T. Burnus, Z. Hu, M. W. Haverkort, J. C. Cezar, D. Flahaut, V. Hardy, A. Maignan, N. B. Brookes, A. Tanaka, H. H. Hsieh, H.-J. Lin, C. T. Chen, and L. H. Tjeng, Phys. Rev. B **74**, 245111 (2006).
[3] Hua Wu, M. W. Haverkort, Z. Hu, D. I. Khomskii, and L. H. Tjeng, Phys. Rev. Lett. **95**, 186401 (2005).
[4] K. Takubo, T. Mizokawa, S. Hirata, J. Y. Son, A. Fujimori, D. Topwal, D. D. Sarma, S. Rayaprol, and E. V. Sampathkumaran, Phys. Rev. B **71**, 073406 (2005).
[5] H. Fjellvåg, E. Gulbrandsen, S. Aasland, A. Olsen, and B. C. Hauback, J. Solid State Chem. **124**, 190 (1996).
[6] A. Maignan, C. Michel, A. C. Masset, C. Martin, and B. Raveau, Eur. Phys. J. B **15**, 657 (2000).
[7] D. Flahaut, A. Maignan, S. Hébert, C. Martin, R. Retoux, and V. Hardy, Phys. Rev. B **70**, 094418 (2004).
[8] S. Aasland, H. Fjellvåg, and B. Hauback, Solid State Commun. **101**, 187 (1997).
[9] O. A. Petrenko, J. Wooldridge, M. R. Lees, P. Manuel, and V. Hardy, Eur. Phys. J. B **47**, 79 (2005).
[10] S. Agrestini, C. Mazzoli, A. Bombardi, and M. R. Lees, Phys. Rev. B **77**, 140403(R) (2008).
[11] S. Agrestini, L. C. Chapon, A. Daoud-Aladine, J. Schefer, A. Gukasov, C. Mazzoli, M. R. Lees, and O. A. Petrenko, Phys. Rev. Lett. **101**, 097207 (2008).
[12] T. Moyoshi and K. Motoya, J. Phys. Soc. Jpn. **80**, 034701 (2011).
[13] Y. Kamiya and C. D. Batista, Phys. Rev. Lett. **109**, 067204 (2012).
[14] S. Agrestini, C. L. Fleck, L. C. Chapon, C. Mazzoli, A. Bombardi, M. R. Lees, and O. A. Petrenko, Phys. Rev. Lett. **106**, 197204 (2011).
[15] H. Kageyama, K. Yoshimura, K. Kosuge, H. Mitamura, and T. Goto, J. Phys. Soc. Jpn. **66**, 1607 (1997).
[16] V. Hardy, M. R. Lees, O. A. Petrenko, D. McK. Paul, D. Flahaut, S. Hébert, and A. Maignan, Phys. Rev. B **70**, 064424 (2004).
[17] A. Maignan, V. Hardy, S. Hébert, M. Drillon, M. R. Lees, O. Petrenko, D. Mc K. Paul, and D. Khomskii, J. Mater. Chem. **14**, 1231 (2004).
[18] C. L. Fleck, M. R. Lees, S. Agrestini, G. J. McIntyre, and O. A. Petrenko, Europhys. Lett. **90**, 67006 (2010).
[19] P. J. Baker, J. S. Lord, and D. Prabhakaran, J. Phys.: Condens. Matter **23**, 306001 (2011).
[20] Xiaoyan Yao, Shuai Dong, Hao Yu, and Junming Liu, Phys. Rev. B **74**, 134421 (2006).
[21] Y. B. Kudasov, Phys. Rev. Lett. **96**, 027212 (2006).
[22] Y. B. Kudasov, Europhys. Lett. **78**, 57005 (2007).
[23] V. Hardy, S. Lambert, M. R. Lees, and D. McK. Paul, Phys. Rev. B **68**, 014424 (2003).
[24] H. Kageyama, K. Yoshimura, K. Kosuge, M. Azuma, M. Takano, H. Mitamura, and T. Goto, J. Phys. Soc. Jpn. **66**, 3996 (1997).
[25] J. A. M. Paddison, S. Agrestini, M. R. Lees, C. L. Fleck, P. P. Deen, A. L. Goodwin, J. R. Stewart, and O. A. Petrenko, arXiv:1312.5243 [cond-mat.str-el].
[26] R. Frésard, C. Laschinger, T. Kopp, and V. Eyert, Phys. Rev. B **69**, 140405(R) (2004).
[27] A. Jain, P. Y. Portnichenko, H. Jang, G. Jackeli, G. Friemel, A. Ivanov, A. Piovano, S. M. Yusuf, B. Keimer, and D. S. Inosov, Phys. Rev. B **88**, 224403 (2013).
[28] G. Allodi, R. De Renzi, S. Agrestini, C. Mazzoli, and M. R. Lees, Phys. Rev. B **83**, 104408 (2011).
[29] R. J. Glauber, J. Math. Phys. **4**, 294 (1963).
[30] M. Suzuki and R. Kubo, J. Phys. Soc. Jpn. **24**, 51 (1968).
[31] M. J. Freiser, Phys. Rev. **123**, 2003 (1961).
[32] L. C. Chapon, Phys. Rev. B **80**, 172405 (2009).